Theta phase resetting and the error-related negativity

NICK YEUNG,[a] RAFAL BOGACZ,[b] CLAY B. HOLROYD,[c] SANDER NIEUWENHUIS,[d] AND
JONATHAN D. COHEN[e]

[a]Department of Psychology, Carnegie Mellon University, Pittsburgh, Pennsylvania, USA
[b]Department of Computer Science, University of Bristol, Bristol, UK
[c]Department of Psychology, University of Victoria, Victoria, British Columbia, Canada
[d]Department of Psychology, Leiden University, Leiden, The Netherlands
[e]Department of Psychology, Princeton University, Princeton, New Jersey, USA

Abstract

It has been proposed that the error-related negativity (ERN) is generated by phase resetting of theta-band EEG oscillations. The present research evaluates a set of analysis methods that have recently been used to provide evidence for this hypothesis. To evaluate these methods, we apply each of them to two simulated data sets: one set that includes theta phase resetting and a second that comprises phasic peaks embedded in EEG noise. The results indicate that the analysis methods do not effectively distinguish between the two simulated data sets. In particular, the simulated data set constructed from phasic peaks, though containing no synchronization of ongoing EEG activity, demonstrates properties previously interpreted as supporting the synchronized oscillation account of the ERN. These findings suggest that the proposed analysis methods cannot provide unambiguous evidence that the ERN is generated by phase resetting of ongoing oscillations.

Descriptors: EEG, ERP, Synchrony, Oscillations, Phase resetting

Monitoring of ongoing performance plays an important role in normal cognitive function: To learn from our mistakes, we must first be able to reliably detect their occurrence. This ability to detect our errors, and more generally to detect performance deteriorations and unfavorable outcomes, has been the object of study for a number of years using both behavioral methods (Rabbitt, 1966, 2002) and neuroimaging techniques (Botvinick, Braver, Carter, Barch, & Cohen, 2001; Carter et al., 1998; Falkenstein, Hohnsbein, Hoorman, & Blanke, 1990; Gehring, Goss, Coles, Meyer, & Donchin, 1993). In particular, a good deal of research has focused on the error-related negativity (ERN), a component of the event-related brain potential that is observed following incorrect responses in simple decision tasks (Falkenstein et al., 1990; Gehring et al., 1993). The ERN is typically found to peak within 100 ms of error commission, suggesting that it may reflect the operation of a neural system for monitoring ongoing behavior.

Competing theories variously propose that the ERN reflects the operation of a dedicated error monitoring system (Falkenstein et al., 1990; Gehring et al., 1993), the arrival of an error signal at the motor system (Holroyd & Coles, 2002),

detection of conflict during response selection (Botvinick et al., 2001; Yeung, Botvinick, & Cohen, 2004), or an emotional response to errors (Bush, Luu, & Posner, 2000; Pailing, Segalowitz, Dywan, & Davies, 2002; Yeung, 2004). However, while most studies to date have focused on the question of the functional significance of the ERN, a second debate has arisen about the nature of neural activity that gives rise to this component. Specifically, whereas many theories appear to assume that the ERN is produced by a sudden phasic burst of activity following detection of an error, Luu and Tucker (2001) have proposed that the ERN may be produced by a reorganization of ongoing oscillatory neural activity that may begin some time prior to incorrect responses. In previous work, we have questioned the strength of the evidence supporting this hypothesis (Yeung, Bogacz, Holroyd, & Cohen, 2004). The aim of the present article is to evaluate a new set of methods recently proposed in support of this hypothesis (Luu, Tucker, & Makeig, 2004).

The debate about the neural basis of the ERN represents an important test case of a wider debate about the relationship between activity in the ongoing electroencephalogram (EEG) and activity in the averaged event-related brain potential (ERP). We have characterized this debate as being between the *classical* and *synchronized oscillation* theories of ERP generation (Yeung, Bogacz et al., 2004). According to the classical view, peaks in ERP waveforms reflect phasic bursts of activity in one or more brain regions that are triggered by experimental events of interest. Specifically, it is assumed that an ERP-like waveform is evoked by each event, but that on any given trial this ERP "signal" is buried in ongoing EEG "noise." In this context, use

of the term EEG "noise" does not imply that the ongoing activity is random or cognitively meaningless, but rather implies that this activity is not correlated with (or time-locked to) the event of interest. Thus defined, EEG noise will tend to average to zero across trials, revealing ERP signals that are consistently time-locked to the event (Coles, Gratton, & Fabiani, 1990; Coles & Rugg, 1995; Goff, Allison, & Vaughan, 1978; Vaughan, 1969).

The classical view therefore treats the ongoing EEG as background noise that obscures the ERP signal of interest, noise that can be dealt with through data averaging. The synchronized oscillation hypothesis—which Luu and Tucker (2001) have applied to the ERN—challenges this approach of treating ERP waveforms as being generated independently of ongoing EEG oscillations. Instead, the hypothesis proposes that ERP peaks are generated when an event leads to resetting of the phase of ongoing EEG oscillations, such that peaks and troughs in the oscillatory waveform become aligned—that is, time-locked to the resetting event (Başar, 1980; Jansen, Agarwal, Hegde, & Boutros, 2003; Klimesch et al., 2004; Makeig et al., 2002; Sayers, Beagley, & Henshall, 1974). When aligned in this way, oscillatory peaks and troughs in the ongoing EEG will be evident in the ERP waveform even in the absence of transient bursts of EEG activity. According to this view, ERP waveforms may not reflect large amplitude, phasic electrophysiological events that occur on individual trials, but may rather reflect modulations of ongoing neural activity that become apparent as synchronized activity in the EEG.

Various pieces of evidence have been presented on either side of this debate (e.g., Brandt, Jansen, & Carbonari, 1991; Klimesch, Hanslmayr, Sauseng, & Gruber, 2006; Kruglikov & Schiff, 2003; Makeig et al., 2002; and Sayers et al., 1974, present evidence of synchronized oscillations, whereas Cooper, Winter, Crow, & Walter, 1965; Mäkinen, Tiitinen, & May, 2005; and Shah et al., 2004, present evidence favoring the classical view). Complicating the debate, there is disagreement about the properties of the EEG and averaged ERP that may be taken as diagnostic of the presence of classical phasic peaks or synchronized oscillations (e.g., see Klimesch et al., 2006; Mäkinen et al., 2005). This issue has become particularly salient in light of recent research using sophisticated analytic techniques to support the synchronized oscillation hypothesis (e.g., Gruber, Klimesch, Sauseng, & Doppelmayr, 2005; Luu & Tucker, 2001; Makeig et al., 2002). Many of these analysis methods seek to demonstrate dependencies of the averaged ERP on properties of the ongoing EEG, on the assumption that such dependencies are a unique prediction of the synchronized oscillation hypothesis. However, as has been frequently noted (e.g., Jervis, Nichols, Johnson, Allen, & Hudson, 1983; Mäkinen et al., 2005; Mazaheri & Picton, 2005; Shah et al., 2004; Yeung, Bogacz et al., 2004), the presence of classical phasic activity will tend to distort the phase and amplitude properties of the EEG. These distortions in many cases mimic properties that might otherwise be taken as diagnostic of the presence of synchronized oscillations.

We have recently used simulations of ERN data (Yeung, Bogacz et al., 2004) to demonstrate this point in relation to some analysis methods that have been used to support the synchronized oscillation hypothesis (Luu & Tucker, 2001; Makeig et al., 2002). In that earlier study, we applied a set of proposed analyses to simulated EEG data that were created according to the classical view, comprising phasic peaks embedded in uncorrelated background EEG noise. The critical finding was that our simulated data, which contained no phase resetting of ongoing EEG

activity, displayed properties that had previously been interpreted as evidence of synchronized oscillations. These findings suggested that the methods proposed by Luu and Tucker (2001) and Makeig et al. (2002) do not provide unambiguous evidence of the presence of synchronized oscillations.

Since our original presentation of this research (Bogacz, Yeung, & Holroyd, 2002; Yeung, Bogacz et al., 2004), and as part of their ongoing research program, Luu and colleagues have proposed an additional set of analysis methods in support of the synchronized oscillation account of the ERN (Luu et al., 2004). Their analyses range from straightforward visual inspection of single-epoch EEG traces to sophisticated analyses of frequency-specific properties of the EEG and averaged ERP. In the present research, we develop our previously reported simulation methods (Yeung, Bogacz et al., 2004) in order to assess the validity of the proposed methods. To this end, we apply each analysis method to three data sets: empirical data from a study of the ERN, simulated data in which the ERN is modeled as arising from synchronization of ongoing EEG theta, and simulated data in which the ERN is modeled as a "classical" phasic peak. More specifically, in the former simulation, we modeled the ERN as arising from phase resetting and enhancement of ongoing EEG theta activity. The enhancement—that is, amplitude increase—of theta activity captures the substantial increase in theta power at the time of the ERN that has been observed empirically (e.g., Luu et al., 2004; Yeung, Bogacz et al., 2004). In the latter simulation, the increase in theta power is explained in terms of the presence of a phasic peak with significant energy in the theta band.[1]

Our experimental logic is the same as in our earlier study: Of interest is whether the analysis methods in question can effectively distinguish between the competing accounts of ERP generation, as exemplified by our two simulated data sets. In this regard, our aim is not to challenge Luu et al.'s claims that the patterns they observe can be explained by the phase resetting view; indeed, as will become clear below, our phase resetting simulation validates these claims. Rather, our aim is to evaluate Luu et al.'s stronger claim that the observed patterns can only be explained in terms of phase resetting and cannot be explained by the classical view. That is, of critical interest is whether findings observed empirically (and in our phase-resetting simulation) can also be observed in our classical peak simulation, which contains no synchronization of ongoing oscillations. If so, then the ability of the proposed methods to provide unambiguous evidence of synchronized oscillations would be called into question.

Methods

Empirical Data

We reanalyzed empirical data used in our previous research (Yeung, Bogacz et al., 2004; Yeung, Botvinick et al., 2004), taken from an experiment in which 16 subjects performed a speeded RT task (Eriksen & Eriksen, 1974). The subjects produced between 31 and 99 errors each during the session ($M = 60.8$). Our analyses focus on the resulting 973 error trials: For each error trial we

---

[1] The observation that the ERN is associated with a large increase in theta power rules out the possibility that this component is generated by "pure phase resetting," that is, phase resetting in the absence of amplitude modulation. This leaves us with the two possible accounts of the neural basis of the ERN—phase resetting with enhancement or a classical phasic peak—that we implemented in our parallel simulations.

extracted a response-locked EEG epoch running from 800 ms before the response until 800 ms after. In all analyses, we discarded the first and last 200 ms of each epoch to avoid contamination from edge artifacts after filtering. Data were collected from 31 electrode positions: FP1, FP2, AFz, F7, F3, Fz, F4, F8, FT7, FC3, FCz, FC4, FT8, T7, C3, Cz, C4, T8, TP7, CP3, CPz, CP4, TP8, P7, P3, Pz, P4, P8, O1, Oz, and O2.

Classical Peak Simulation

This simulation developed the methods introduced by Yeung, Bogacz et al. (2004), in which EEG data are simulated by adding phasic ERP peaks to background EEG "noise." Two phasic peaks were used: a sharp negative deflection (corresponding to the ERN) and a positive-going slow wave (corresponding to the Pe, a centroparietal positivity often observed to follow the ERN). The simulated background EEG was constructed by summing together a number of phase-randomized sinusoids, the amplitude of which varied with frequency according to the power spectrum of empirical EEG data. This process amounts to an inverse-Fourier transformation with randomized phase, and is thus effective in matching the surface features of the empirical EEG data.

In our previous research, we used a single set of simulation parameters to fit the entire 973-epoch data set. In the present research, the analyses of interest included some that were applied to single subject data. We therefore fit each individual subject's ERP data separately. The procedure for each subject, illustrated in Figure 1, was as follows. Starting with the averaged ERP of a particular subject (Figure 1a), we first identified the slow-wave component that minimized mean squared error—as a function

of frequency, peak latency, and amplitude—relative to the empirical ERP across the −600 to +600-ms epoch (Figure 1b). We next fit the ERN peak as a latency-jittered, half cycle of a 6-Hz sinusoid (Figure 1c, gray lines). Latency jitter across trials results in a peak in the averaged ERP that is of lower frequency and lower amplitude than the phasic peaks present in individual epochs (Figure 1c, black line). The standard deviation of latency jitter of the phasic peak, together with its peak amplitude and mean latency, were again selected to minimize mean squared error relative to the empirical ERP. Together, the slow-wave component and jittered phasic peak accurately capture the principal features of the empirical ERP data (Figure 1d).

Using this method, the data were first fit to the averaged ERP of each subject from electrode FCz, at which the ERN is maximal. Across subjects, parameter values at this location for the slow-wave component were: mean frequency = 0.9 Hz (range = 0.7–1.3 Hz); mean peak latency = 244 ms (range = 100–404 ms); mean amplitude = 20 μV (range = 10–34 μV). Parameter values for the phasic peak were: mean latency jitter = 29 ms (range = 20–40 ms); mean peak latency = 65 ms (range = 44–92 ms); mean amplitude = 26 μV (range = 9–47 μV). Once we had fit parameters of the phasic peaks for the averaged ERP at electrode FCz, we then generated ERP peaks for each of the other 30 simulated electrode locations. As in our previous research (Yeung, Bogacz et al., 2004), the simulated scalp distribution of each component was simulated using a forward model algorithm that assumes a point source for each component (BESA 2000; www.besa.de). The phasic peak had a midline frontocentral scalp distribution, whereas the slow-wave component had a midline centroparietal distribution.
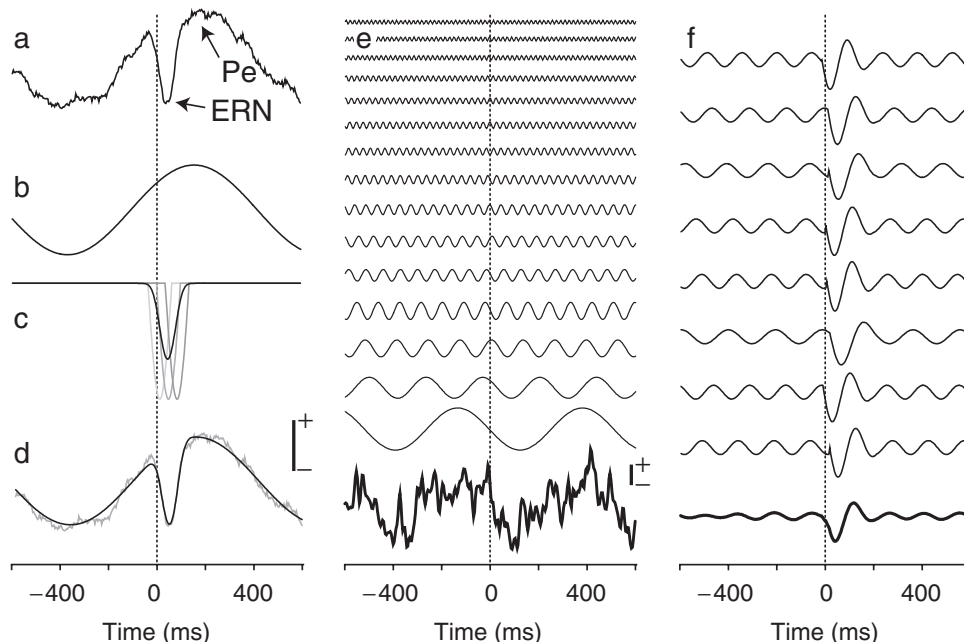
Figure 1. Construction of the simulated ERP. a: Averaged ERP for one sample subject from electrode FCz. b: A slow-wave component was fit to the empirical data to minimize mean squared error as a function of frequency, phase, and amplitude. c: In the classical peak simulation, the ERN was modeled as a latency jittered half-cycle of a 6-Hz sinusoid. Latency jitter causes the peak evident in the averaged ERP (black line) to have lower frequency and amplitude than the peaks present on individual trials (gray lines). d: The simple two-component model provides a good fit to the empirically observed ERP. e: The background EEG is simulated by summing together sinusoids of random phase and frequency, scaled to match the power spectrum of empirical EEG data. f: In the phase resetting simulation, the ERN was modeled by resetting the phase and increasing the amplitude of ongoing theta activity in the EEG. The thin black lines plot theta activity in individual epochs, in which a sharp phase transition and amplitude increase is apparent. The thick black line plots the average of these individual epochs, in which the simulated ERN is clearly evident.

After simulating phasic components for 973 epochs at each of the 31 electrode locations, we next added simulated EEG noise. As described above, the background EEG was simulated by summing together sinusoids of randomly varying frequency and phase, the amplitudes of which were scaled to match the power spectrum of empirical EEG data (Figure 1e). We summed 50 sinusoids, ranging in frequency from 0.1 to 125 Hz, to create each simulated EEG epoch. The maximum amplitude of any single sinusoid (at 0.1 Hz) was 20 μV. For each subject, we generated as many EEG epochs as there were error trials in the empirical data for that subject. The simulated data set therefore comprised 16 simulated "subjects" of data, with 31–99 ($M = 60.8$) EEG epochs per subject, each running from −800 ms to +800 ms relative to the response. The simulated data were subjected to identical analyses as the empirical EEG data.

Phase Resetting Simulation

An additional simulated data set was created to implement the synchronized oscillation account of the ERN. The methods used in this simulation were very similar to those described above for the classical peak simulation. The sole difference was that the ERN was modeled by phase resetting and enhancement of on-going theta activity in the EEG, rather than as a superimposed peak that is independent of this ongoing activity. Each simulated epoch thus included theta activity with initial random phase. At around 0 ms, the phase of this theta oscillation was abruptly reset and its amplitude sharply increased for a fixed duration (cf. Klimesch et al., 2006; Mäkinen et al., 2005). As noted above, theta enhancement is needed to simulate the empirically observed increase in theta power associated with the ERN (i.e., the data cannot be simulated accurately in terms of "pure phase reset-ting"; Yeung, Bogacz et al., 2004). Sample trials of theta activity are illustrated in Figure 1f (thin black lines). Phase resetting and enhancement leads to the alignment of large peaks and troughs across trials, such that the averaged ERP (Figure 1f, thick black line) is marked by a sharp negative deflection peaking at the latency of the ERN.

The frequency of theta activity was randomly selected on each trial to take a value from 4 to 8 Hz (mean = 6 Hz). Three other simulation parameters were selected to maximize the fit to the empirical EEG data at electrode FCz: mean phase resetting latency = 32 ms (range = 20–60 ms), mean latency jitter = 25 ms (range = 18–32 ms), and mean theta amplitude after enhance-ment = 25 μV (range = 11–43 μV). As was the case for the classical peak simulation, ERN-related activity was combined with a Pe component—with both scaled appropriately across the 31 simulated electrode locations—and then combined with (non-theta) EEG activity. Overall, the simulation com-prised 16 "subjects" of data, for a total of 973 simulated EEG epochs, each running from −800 ms to +800 ms relative to the response.

Simulation and Analysis Methods

The simulated data were generated using Matlab (The Math-works, Inc.) algorithms that are available online (http://www.cs.bris.ac.uk/home/rafal/phasereset/). Data analyses were performed in Matlab using EEGLab software (http://www.sccn.ucsd.edu/eeglab) and custom algorithms. Filtering used the EEGLab function "eegfilt," implementing a two-way least-squares finite impulse response filter with zero phase shift, 3-dB attenuation at cutoff frequencies, and 1-Hz transition bands.

Results

Luu et al. (2004) describe a number of new analysis methods, the results of which they interpret as favoring the hypothesis that the ERN is generated by phase resetting of theta (4–7 Hz) activity in medial frontal cortex. Their analyses aim to identify properties of the EEG and averaged ERP within this frequency band that may be taken as diagnostic of the presence of synchronized oscilla-tions. In what follows, we apply their methods to our empirical and simulated data sets. Our aim in doing so is to determine whether these analysis methods are capable of distinguishing be-tween the competing accounts of the ERN. Given this aim, the critical question is whether properties observed in the empirical data are uniquely observed in the phase resetting simulation, as Luu et al.'s interpretation would predict, or whether correspond-ing properties can also be observed in the classical peak simu-lation (that contains no phase resetting).
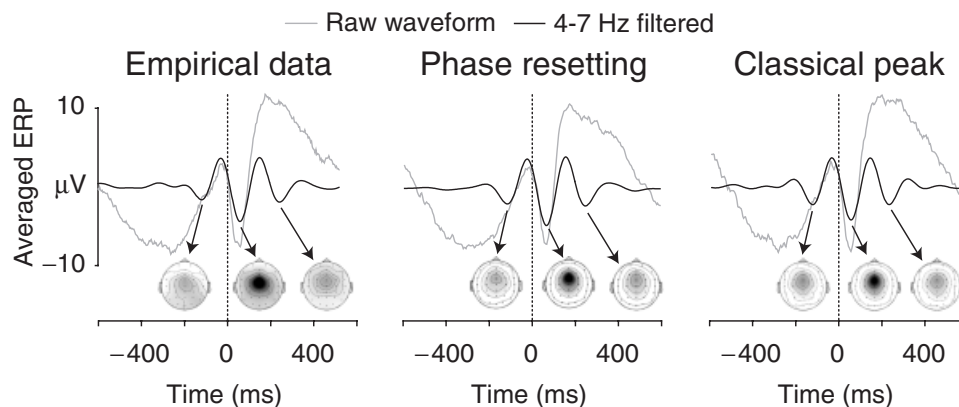
Figure 2. Averaged ERPs. Response-locked ERP waveforms from electrode FCz for empirical data (left panel), simulated data with theta phase resetting (middle panel), and simulated data with a classical phasic peak (right panel). Separate waveforms are shown for unfiltered and 4–7-Hz filtered data (gray and black lines, respectively). Scalp plots indicate the topography at the time of each of the three negative peaks evident in the filtered waveforms.

Basic Features

Grand-averaged ERP waveforms for the empirical and simulated data at electrode FCz are shown in Figure 2 (gray lines), together with 4–7-Hz filtered waveforms (black lines). For the empirical data, the unfiltered ERP is characterized by a sharp negative component, peaking $\sim$ 64 ms postresponse, that is superimposed on a slow positive-going component. The negative and positive peaks correspond to the ERN and Pe, respectively. The low-frequency Pe component is removed by 4–7-Hz filtering (black line), but the filtered waveform shows a clear peak corresponding to the ERN that is maximal 68 ms after the response. In this filtered waveform, the ERN peak is flanked by smaller negative peaks at -112 ms and $+252$ ms. The three negative peaks in the filtered waveform share a frontocentral scalp topography. Comparing the raw and 4–7-Hz filtered waveforms, it is clear that much of the power of the ERN is concentrated at the theta frequency: The 4–7-Hz filtered waveform accounts for most (74%) of ERN peak amplitude in the unfiltered waveform.

As shown in the center and right-hand panels of Figure 2, all of these key features of the empirical data are replicated in both the phase resetting and classical peak simulations. Given that each simulation was constructed to match the raw empirical data, it is unsurprising that the unfiltered waveforms (gray lines) replicate the empirical pattern of a sharp ERN component that is superimposed on a slow positive-going component. It is also unsurprising that the ERN appears as part of a sustained theta oscillation in the filtered phase resetting simulation (Figure 2, middle panel, black line). However, of much greater interest is the observation that the temporal and spatial properties of theta activity observed in the empirical data are also replicated in the classical peak simulation (Figure 2, right panel). Thus, the 4–7-Hz filtered ERP waveform (black line) is characterized by apparent oscillatory activity that has a peak amplitude at the latency of the ERN (64 ms postresponse). Flanking this peak are negativities at -120 ms and $+244$ ms that share the frontocentral scalp topography of the ERN. Theta activity accounts for most (66%) of the amplitude of the ERN evident in the unfiltered waveform.

The presence of oscillatory features in the filtered classical peak data may initially seem surprising, given that these data are constructed from phasic peaks embedded in phase-random noise. These oscillatory features are, in fact, ringing artifacts that are created by filtering of the simulated phasic ERN peak. The origin of these ringing artifacts is illustrated in Figure 3, which presents a frequency-based decomposition of the phasic peak used to simulate the ERN. As shown in Figure 3, the phasic peak contains energy in a range of frequency bands. Within each frequency band, there is a central peak that is flanked by side oscillations. When summed across all frequency bands, the side oscillations cancel to leave only the central phasic peak.

The application of a 4–7-Hz bandpass filter, which effectively removes activity at lower and higher frequencies, results in the appearance of theta-frequency oscillations that begin long before the onset of the phasic peak and continue long after its offset. Thus, in the theta filtered component (see Figure 3), the ERN is preceded and followed by artifactual peaks at $\pm$ 88 ms (positive peaks, 82% amplitude of the ERN), $\pm$ 172 ms (negative peaks, 45% amplitude), and $\pm$ 264 ms (positive peaks, 13% amplitude). In this way, narrow bandpass filtering distorts the amplitude and latency estimates of theta activity to create the
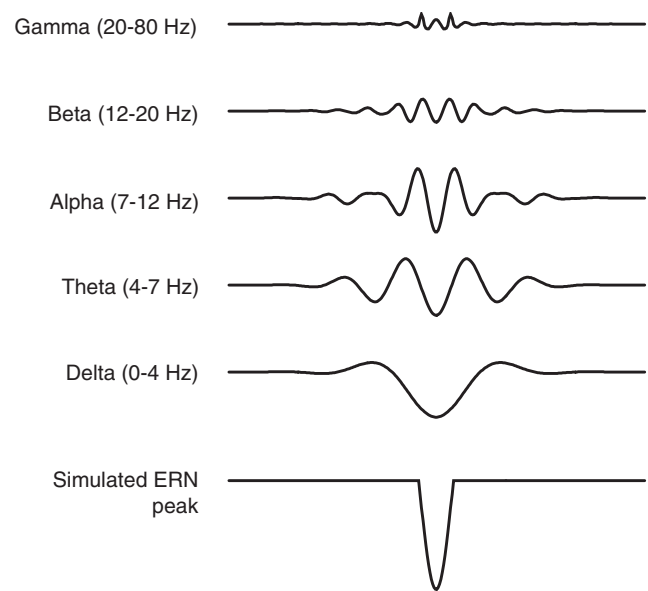

Figure 3. Frequency composition of the simulated classical peak. The simulated phasic peak contains appreciable energy in a wide range of EEG frequency bands. Oscillatory activity within each narrow frequency range extends well beyond the onset and offset of the original phasic peak.

appearance of oscillatory features where none are present in the data (cf. Yeung, Bogacz et al., 2004). As discussed in detail below, the presence of these ringing artifacts plays a key role in explaining why our classical peak simulation, which contains no synchronized oscillations, demonstrates properties that were identified by Luu et al. (2004) as providing evidence that the ERN is generated by theta phase resetting.

Theta Activity in Individual EEG Epochs

Luu et al.'s (2004) first analysis focused on qualitative features of single-trial EEG data. According to the synchronized oscillation hypothesis, the ERN is generated when phase-random theta activity in the EEG becomes synchronized for a brief period. This hypothesis predicts that error-trial EEG epochs should be characterized by phase-random theta prior to the response (reflecting ongoing EEG activity) and phase-coherent theta immediately afterward (reflecting phase resetting of this activity).

Luu et al. (2004) found that these predictions were borne out in a visual inspection of their empirical ERN data. Corresponding patterns are evident in our empirical data, as shown in Figure 4 (left panel), which presents 10 randomly selected single-trial epochs, with overlapping traces for unfiltered (gray lines) and 4–7-Hz filtered (black lines) epochs. Figure 4 shows that individual EEG epochs contain appreciable theta activity prior to the response (e.g., traces E2 and E6), but that the phase of this activity is inconsistent across trials. However, a negative-going EEG deflection is evident on most trials following the response. The negative peak is clearly evident in the 4–7-Hz filtered data, demonstrating that the ERN present on individual trials contains appreciable theta power. The consistency of this peak across trials demonstrates the phase consistency of theta power at this time. Luu et al. suggest that these findings support the notion that the ERN is produced by resetting of theta oscillations in the ongoing EEG. Apparently consistent with this interpretation, corresponding patterns are evident in our phase resetting simulation (Figure 4, middle panel), in which epochs are marked by
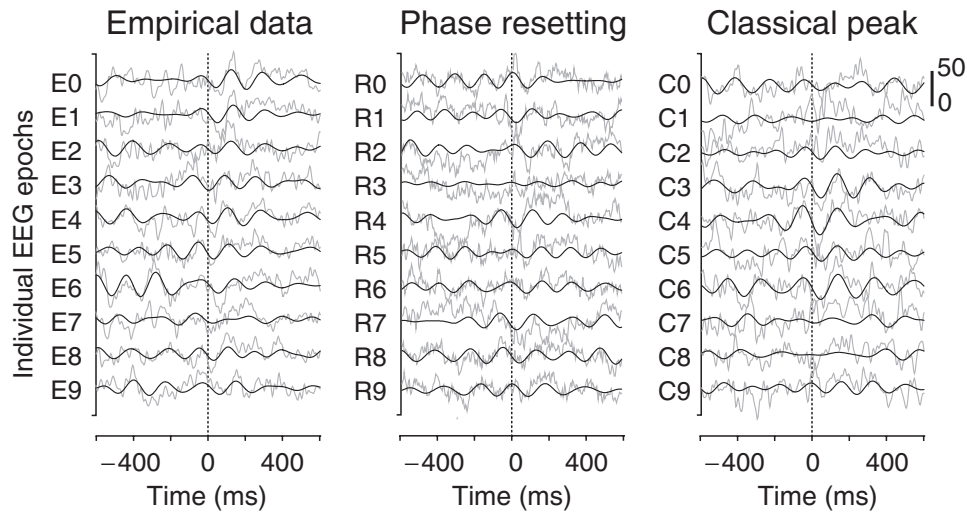
Figure 4. Single-trial EEG data at FCz. Ten randomly selected response-locked EEG epochs are shown for the empirical data (left panel), for the simulated data with theta phase resetting (middle panel), and for the simulated data with a classical phasic peak (right panel). Corresponding unfiltered (gray) and 4–7-Hz filtered (black) waveforms are presented for each epoch.

phase-inconsistent theta prior to the response (e.g., traces R0, R1, R5, R6, and R8) and a consistent negative deflection just afterward.

However, our classical peak simulation shows comparable patterns, despite containing no theta phase resetting (Figure 4, right panel): Individual simulated epochs show clear evidence of theta activity prior to the response (e.g., traces C0, C6, and C7), but with no coherence of phase, whereas a consistent negative deflection with appreciable theta power is present after the response on most trials. The classical peak simulation thus replicates critical properties of the empirical data. Indeed, the simulated data accurately capture the variety of patterns of pre- and postresponse theta activity seen in the empirical data: traces with little theta prior to the response but a burst of theta immediately thereafter (E0; C3), traces with higher theta prior to the response than afterward (E6, E9; C0, C7), traces with consistent theta throughout (E2, E8; C5, C6), and traces with low theta throughout (E7; C8). Given that all of these patterns are apparent in simulated data that contain no synchronized oscillations, it follows that none of them can provide unambiguous evidence of synchronized theta oscillations.

Various patterns are evident in the classical peak simulation even though each epoch is constructed in the same way (by summing together the ERP "signal" with randomized EEG "noise"). The variety emerges from variability in the phase and amplitude of theta activity in the background EEG, which affects how the background EEG summates with or cancels out the phasic ERN peak. Thus, on some trials the phasic peak happens to coincide with a burst of theta activity in the background EEG. If the peak and background EEG are in phase, such that peaks and troughs in the ongoing EEG are aligned with the phasic peak (and, in the filtered data, with the oscillatory ringing artifact), a large ERN peak will be apparent that will appear as part of an ongoing theta oscillation (e.g., trace C4). Conversely, if the peak and background EEG are out of phase, there may be no peak at all (e.g., trace C1). On other trials, background theta activity may be consistently low throughout the epoch, in which case the ERN will be evident as a sudden burst of theta energy around the time of the response (e.g., trace C2). Background theta may likewise be consistently high, in which case the ERN will appear as part of a prolonged theta oscillation (e.g., trace C6). In this way, various patterns of theta activity can result from the sum-
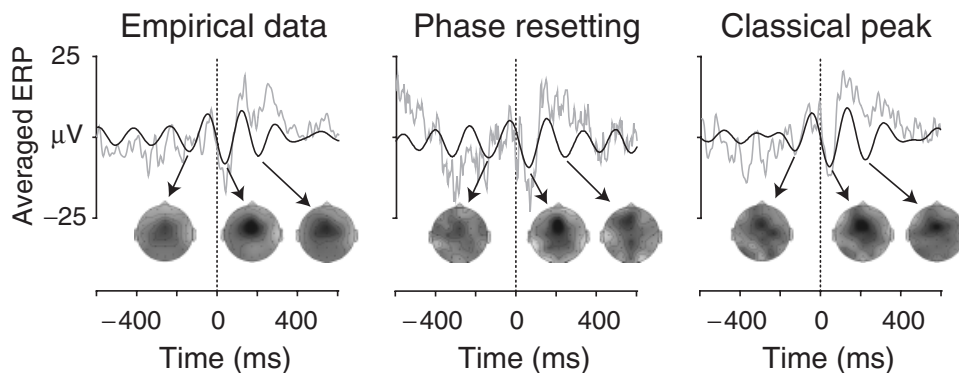
Figure 5. Averaged ERP of single-trial EEG data. Response-locked ERP waveforms from electrode FCz are shown for the empirical and simulated epochs shown in Figure 4, showing raw and 4–7-Hz filtered waveforms (gray and black lines, respectively). Scalp plots indicate the topography at the time of each of the three negative peaks evident in the filtered waveforms.
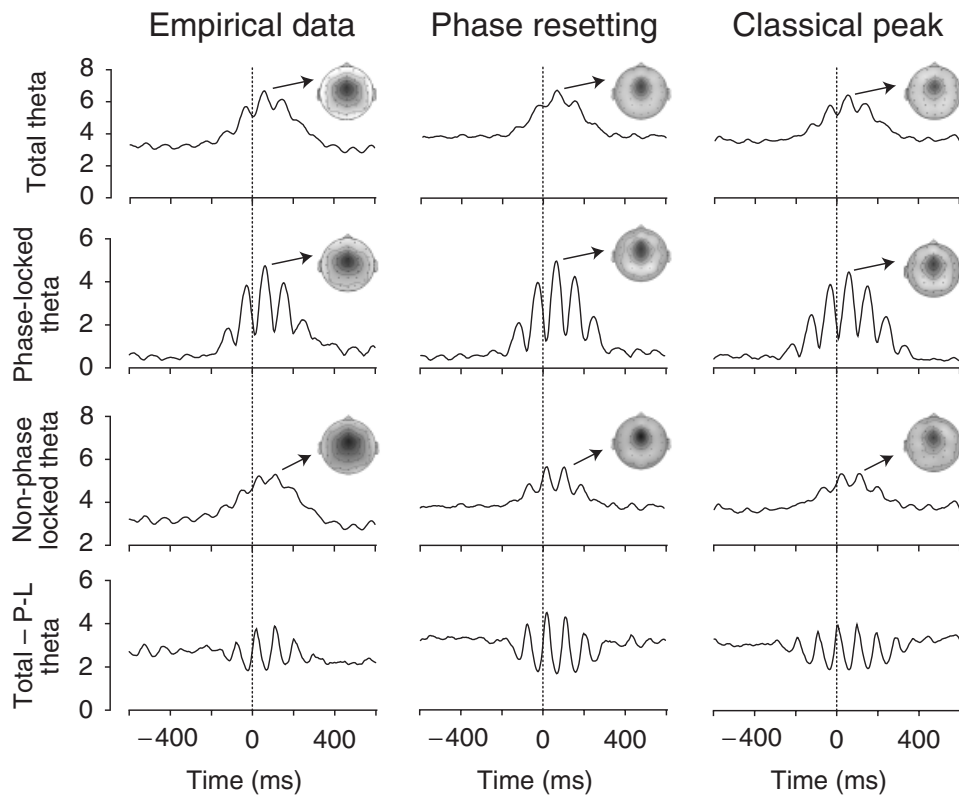
Figure 6. Spatiotemporal properties of theta activity. Plots show the time course of total theta, phase-locked theta, non-phase-locked theta, and the difference between total and phase-locked theta at electrode FCz for the empirical data (left panels), the phase resetting simulation (middle panels), and the classical peak simulation (right panel). Scalp plots show the distribution of theta activity at the maximum of each time course.

mation of a time-locked phasic peak with uncorrelated background noise, and none of these patterns are diagnostic of the presence of synchronized oscillations.

Theta Activity in Averaged ERPs

Figure 5 plots ERP waveforms created by averaging together the 10 individual EEG epochs illustrated in Figure 4. As noted by Luu et al. (2004), the ERN peak coincides with a period during which theta activity in individual EEG epochs is consistent across trials (contrast the left panels of Figures 4 and 5). Thus, although intermittent theta activity is evident in single epochs prior to the response, the inconsistent phase of this activity ensures that it tends to cancel out across trials. For this reason, the amplitude of theta activity is low prior to the response in the 10-trial averaged ERP. In contrast, because there is phase-coherent theta activity immediately following the response, theta activity is correspondingly large in the 10-trial averaged ERP at this time. This theta activity accounts for much of the ERN peak that is apparent in the unfiltered empirical waveform (left panel of Figure 5, gray line). Therefore, the ERN coincides with a period of theta phase coherence in the single-trial EEG data. This result has been interpreted by Luu et al. (2004) as support for the synchronized oscillation account of the ERN, a conclusion apparently supported by the observation of corresponding patterns in our phase resetting simulation (Figures 4 and 5, middle panels).

However, our classical peak simulation also replicates the properties evident in the empirical data (Figures 4 and 5, right panels), demonstrating that these properties are equally consistent with the classical view of ERP generation. As discussed previously (Jervis et al., 1983; Mäkinen et al., 2005; Yeung, Bogacz et al., 2004), adding a phasic peak to EEG noise is equivalent to adding phase-coherent (time-locked) activity at all frequencies contained within the peak. The presence of a phasic peak will therefore tend to concentrate EEG phase toward the phase of the added peak. In the classical peak simulation, the addition of a time-locked phasic 6-Hz peak causes a concentration of phase (and hence a significant ERP peak) in the theta frequency range during the period of the ERN, without affecting or interacting with oscillatory activity in the background EEG. That is, these simulated data demonstrate phase consistency without phase resetting. Thus, although it is true by definition that activity present in the averaged ERP reflects activity in individual EEG epochs that is (partially) phase-locked to the experimental event of interest, it does not follow from this statement that the observed phase *coherence* must be created by phase *resetting* of ongoing EEG oscillations.

Total Theta and Phase-Locked Theta EEG Activity

In addition to analyzing qualitative features of EEG and ERP data, Luu et al. (2004) performed more quantitative analyses of theta activity related to the ERN. Their analysis again focused on the hypothesis that the ERN is generated by increases in theta power and theta phase synchrony. To test this hypothesis, they calculated measures of "total theta" and "phase-locked theta." Total theta provides a measure of the amount of theta in single-trial EEG data, and was calculated by 4–7-Hz filtering and

rectifying (i.e., taking the absolute value of) the data from individual EEG epochs, then averaging across trials and subjects. Phase-locked theta provides a measure of activity that is specifically time-locked to incorrect responses and was calculated by 4–7-Hz filtering and rectifying the averaged ERP from each subject and then averaging across subjects. The results of these analyses applied to our empirical data are plotted in Figure 6 (upper left panels).

Consistent with the findings of Luu et al., our empirical data exhibit sustained and substantial increases in total and phase-locked theta that emerge around the time of the response and peak shortly thereafter (at latency of the ERN). The scalloped form of these measures reflects the partial phase consistency of theta activity across trials. This scalloping is less evident in the total theta measure, which is based on theta activity in individual EEG epochs, because there is appreciable EEG theta activity that is not strongly time-locked to the incorrect response (so that theta activity is high even in the troughs). Critically, the measures of total and phase-locked theta both show marked increases that begin well before the onset of the ERN observed in the unfiltered ERP waveform and extend well beyond its offset, suggesting that the ERN is associated with a long-lasting increase in theta power rather than a transient burst of activity. Luu et al. (2004) interpret these patterns as evidence in support of the synchronized oscillation account of the ERN.

Once again, however, the pattern of results seen in the empirical data is replicated in both of our simulated data sets (Figure 6, middle and right panels), suggesting that this pattern does not distinguish between the phase resetting and classical views. In particular, these findings challenge Luu et al.'s (2004) conclusion that the observed pattern of empirical results uniquely supports the synchronized oscillation account of the ERN. It is particularly striking that total theta activity appears to increase prior to the response in the classical peak simulation, given that the phasic peak occurred after the response in each simulated epoch. To explain this finding, we refer back to the point that narrow-band filtering can produce ringing artifacts (cf. Yeung, Bogacz et al., 2004). In the classical peak simulation, filtering of the ERN results in artifactual ''oscillations'' that extend well before and after the original peak (Figure 3). These ringing artifacts are reflected in a straightforward way in measures of phase-locked theta (which are simply plots of rectified ERP waveforms). The ringing artifacts are also present in individual simulated EEG epochs (Figure 4, right panel), although here they are harder to discern because they are small relative to the amplitude of theta activity in the background EEG. These artifacts are nevertheless present, and result in the appearance of a sustained increase in total EEG theta activity that extends well beyond the edges of the original phasic peak. Thus, the observation of a sustained increase in total and phase-locked theta does not provide unambiguous evidence that the ERN is generated by synchronization of ongoing theta oscillations.

Although not a focus of Luu et al.'s (2004) original analysis, it is noteworthy that they found an asymmetric increase in total theta power in their empirical data. That is, in their data, the increase in theta power began only 200 ms prior to the peak of the ERN but persisted for roughly 400 ms after the peak. Our empirical data do not replicate this asymmetry: As shown in Figure 6, increases in total theta were evident from approximately −200 ms to +300 ms relative to the response; that is, the increase was apparent for roughly 250 ms both before and after the ERN peak. The cause of this discrepancy between our em-

pirical results and those of Luu et al. is unclear. Nonetheless, in this context it is worth noting that neither of the two accounts of ERP generation predicts that increases in theta power must necessarily have a symmetric distribution around the peak latency of the ERN. Instead, the degree of skew in theta power depends on the latency distribution of phase resetting or of the phasic peak. Theta power was symmetrical in the present simulations because we modeled the latencies of phase resetting and phasic peaks with a symmetric (normal) distribution. However, in simulations not reported here, we have replicated Luu et al.'s observed asymmetrical distribution of theta power through the use of skewed (exponential and ex-Gaussian) latency distributions. It follows that the observation of an asymmetric increase in theta power in empirical EEG data (e.g., Luu et al., 2004) does not distinguish between competing theories of the generation of the ERN.

Non-Phase-Locked Theta Activity in the EEG

According to the classical view, the ERN is generated independently of the ongoing EEG. Therefore, in this view there is no reason to expect any relationship between theta activity in the averaged ERP and theta activity in the ''background'' EEG. To assess whether the averaged ERP and background EEG are indeed independent in this way, Luu et al. (2004) calculated a measure of ''non-phase-locked theta'' in their ERN data. Specifically, they calculated non-phase-locked theta by subtracting each subject's averaged ERP from their individual EEG epochs—to remove the contribution of phase-locked activity—then filtering, rectifying, and grand-averaging the resulting data (to reveal the residual, non-phase-locked theta). Figure 6 (lower middle panels) presents analyses of non-phase-locked theta in the empirical and simulated data.

In contrast to the results reported by Luu et al. (2004), our data exhibit a marked, long-lasting increase in non-phase-locked theta around the time of the response. Luu et al. found that non-phase-locked theta showed a sharply scalloped pattern, very similar to the pattern we observe when we subtract phase-locked theta from total theta (Figure 6, left lower panel), suggesting that there may be procedural differences between their study and ours. Despite these differences, critical features are shared by our empirical data and those of Luu et al. Specifically, like Luu et al., we find that non-phase-locked theta activity shows scalloping at the theta frequency that mirrors the scalloping evident in phase-locked theta. Moreover, non-phase-locked and phase-locked theta share a clear frontocentral scalp topography.

Luu et al. argue that this pattern of data supports the synchronized oscillation account of the ERN. Their argument is as follows: If the classical view is correct, and the ERN is generated independently of the ongoing EEG, then there should be no relationship between theta activity in the averaged ERP and ''background'' EEG. However, examination of theta activity reflected in the averaged ERP (phase-locked theta) and in the background EEG (non-phase-locked theta) reveals a close dependence in terms of shared spatiotemporal properties. Luu et al. therefore interpret their findings as supporting the synchronized oscillation account of the ERN. Apparently consistent with this conclusion, analysis of our phase resetting simulation reveals similar patterns (Figure 6, lower middle panels).

However, the patterns evident in the empirical data and phase resetting simulation are once again also evident in our classical peak simulation (Figure 6, right panel), in which the ERP reflects activity that is independent of the background EEG. To under-

stand why these patterns are evident in the classical peak simulation, the critical point to note is that the phasic ERN peak was simulated with a degree of latency variability across trials. Latency variability is inevitably observed in real experimental data (Truccolo, Ding, Knuth, Nakamura, & Bressler, 2002), and has the consequence that the averaged ERP is an imperfect reflection of activity occurring on individual trials (Mazaheri & Picton, 2005; McFarland & Cacace, 2004). In our classical peak simulation, latency jitter introduces temporal smearing that reduces the frequency and amplitude of the averaged peak relative to the peak added on individual trials (Figure 1c). As a consequence, subtracting the averaged ERP from individual trials does not fully remove all of the phasic activity that was added to the background EEG on each trial (i.e., to simulate the ERN under the classical view). Residual phasic activity therefore contaminates the measure of non-phase-locked activity. This contamination accounts for the close relationship between phase-locked and non-phase-locked theta activity that is evident in classical peak simulation—both reflect the spatiotemporal properties of the added phasic peak—and demonstrates that this close relationship is not a unique prediction of the synchronized oscillation hypothesis.

Scalp Distribution of Theta Activity

Spatiotemporal properties of the empirical and simulated data are illustrated in Figures 2, 5, and 6. Our empirical data demonstrate important properties that Luu et al. (2004) have interpreted as being inconsistent with a classical view account of the ERN. First, the oscillatory features evident in the 4–7-Hz filtered ERP (Figures 2 and 5, left panels) show a consistent frontocentral scalp topography. Luu et al. suggest that, for the classical view to explain the presence of these oscillatory peaks (at -112 ms, 68 ms, and $+252$ ms), one would need to assume that they reflect a sequence of independent phasic events that by chance happen to occur at the theta frequency. As Luu et al. note, if these peaks reflect independent events, then there is no reason to expect them to show a consistent scalp topography or neural source. However, when Luu et al. performed dipole source modeling of their filtered ERP data, they found that the same fixed dipole sources contributed to all of the oscillatory peaks (and hence that these fixed sources showed oscillatory features). A second important property of the empirical data is illustrated in Figure 6 (left panel): Measures of phase-locked and non-phase-locked theta demonstrate a shared frontocentral scalp topography. Luu et al. interpret this close association between measures associated with the averaged ERP (phase-locked theta) and ongoing EEG (non-phase-locked theta) as evidence in favor of the phase-resetting account of the ERN. This close association is indeed apparent in our phase resetting simulation (Figures 2, 5, and 6, middle panels).

However, corresponding analyses of our classical peak simulation suggest that these features are equally consistent with the classical view. Oscillatory features in the simulated ERP show a consistent frontocentral scalp topography (Figures 2 and 5, right panels), as do measures of both phase-locked and non-phase-locked theta activity (Figure 6, right panel). A first implication of these results is that the classical view need not attribute oscillatory features in the filtered ERP to successive, independent phasic peaks. Instead, the presence of oscillatory features in the simulated data is due to ringing artifact associated with narrow bandpass filtering of a single phasic peak that manifests as a series of regularly spaced (oscillatory) peaks (Figure 3). Critically, the amplitude of the ringing artifact varies across scalp locations in proportion to the size of the original peak, and hence the artifactual oscillations show a consistent scalp topography. Modeling the neural source of these (artifactual) oscillations would necessarily reveal fixed sources with oscillatory features, even though the original peak was generated according to the classical view. It follows that the empirically observed pattern—of oscillatory features with consistent scalp topography and neural source—does not provide unambiguous evidence of synchronized oscillations; this pattern may also be produced when narrow bandpass filtering causes ringing artifacts around a phasic peak.

Figure 6 (right panel) shows that the classical peak simulation also replicates the empirically observed pattern of a consistent scalp topography of phase-locked and non-phase-locked theta. Phase-locked theta reflects in a straightforward way the addition of the phasic ERN peak, and therefore replicates the (frontocentral) scalp topography of this peak. Of more interest is the observation of the same topography in non-phase-locked theta. Luu et al. (2004) suggest that the classical view would not predict this finding, because subtracting the averaged ERP from EEG data should isolate uncorrelated EEG noise that is independent of the phasic peak. However, as noted above, to the extent that there is any latency jitter of phasic events present in the EEG, the averaged ERP will be an imperfect reflection of phasic activity occurring on individual trials. Hence, subtracting the averaged ERP will never be completely effective in isolating the "background" EEG: There will always be some contamination from phasic activity that is not subtracted out. In the classical peak simulation, the substantial increase in non-phase-locked theta (Figure 6, lower right panels) is entirely attributable to this residual phasic activity. Non-phase-locked theta therefore shares a common scalp topography with phase-locked theta in the classical peak simulation, because both reflect the properties of the added phasic peak.

Discussion

We have used simulations of EEG data to evaluate a set of sophisticated analysis methods used by Luu et al. (2004) to support the hypothesis that the ERN is generated by synchronization of ongoing theta oscillations in the EEG. The simulation results call into question whether these methods can provide unambiguous evidence on this issue. In each case, patterns evident in the empirical data were equally evident in both the phase resetting and classical peak simulations. These findings suggest that the proposed analysis methods do not effectively disambiguate between competing accounts of the neural basis of the ERN. In particular, it is striking that our classical peak simulation—which contained no phase resetting of ongoing EEG activity—demonstrated all of the properties that Luu et al. had taken to be diagnostic of the presence of synchronized oscillations.

An important implication of our findings is that there may be only subtle differences between the predictions of the classical and synchronized oscillation hypotheses, and that it may not be possible to distinguish the accounts on the basis of broad, qualitative features of the data. In their analyses, Luu et al. (2004) identified the following properties as being diagnostic of the presence of theta phase resetting: (1) the presence of oscillatory features in narrow bandpass filtered ERP and EEG data, (2) the consistent scalp topography and neural source of these

oscillatory features, (3) the association between theta power in the ERP and phase-coherent theta activity in individual EEG epochs, and (4) the shared scalp topography and neural source of phase-locked and non-phase-locked theta EEG activity. We do not dispute Luu et al.'s claim that their phase-resetting account can explain the observation of these properties in empirical studies. Indeed, our simulations of the phase-resetting view support this claim. However, our simulations demonstrate that each of the observed properties is equally consistent with the classical view of the ERN as arising from phasic neural activity occurring independently of ongoing EEG processes.

As we have discussed previously (Yeung, Bogacz et al., 2004), narrow bandpass filtering necessarily results in the observation of oscillatory features in the frequency range of interest (property 1). In the present classical peak simulation, 4–7-Hz filtering of a phasic ERP peak resulted in ringing artifacts that very closely resembled oscillatory features observed in empirical data. These ringing artifacts were also present in individual simulated epochs, where they summed or canceled with theta activity in the background EEG in ways that closely mimicked patterns evident through visual inspection of empirical EEG data. Moreover, because the oscillatory features of the simulated data were caused by ringing artifacts, their spatiotemporal properties reflected those of the phasic peak used to simulate the ERN (property 2).

Our classical peak simulation also demonstrated a clear association between the ERN and phase-coherent theta activity (property 3). Thus, although it is true that the presence of theta power in the averaged ERP indicates that there is phase-coherent activity in individual EEG epochs—if theta activity was not coherent, it would tend to average to zero across trials—it does not follow that this phase coherence must be produced by synchronization of ongoing oscillations. That is, the observation of phase *coherence* does not necessarily imply the presence of phase *resetting* (Jervis et al., 1983; Mäkinen et al., 2005; Yeung, Bogacz et al., 2004). As our simulations demonstrate, theta phase coherence is also a necessary consequence of adding event-related phasic peaks with energy in the theta frequency range. Therefore, analyses that simply seek to demonstrate the presence of phase coherence cannot distinguish the competing accounts: The critical requirement is to identify the specific cause of this coherence.

Finally, phase-locked and non-phase-locked theta activity in the classical peak simulation shared a common frontocentral scalp distribution (property 4). This pattern was observed because subtracting the averaged ERP—as part of the calculation of non-phase-locked theta—does not effectively remove the contribution of phasic activity to the EEG. Latency variability means that the averaged ERP underestimates the frequency and amplitude characteristics of phasic activity in individual EEG epochs (Mazaheri & Picton, 2005; McFarland & Cacace, 2004; Truccolo et al., 2002). Residual phasic activity will therefore contaminate measures of the "background" EEG even after the averaged ERP is subtracted from each trial. Hence, even if the classical view were correct, one would expect measures of non-phase-locked theta activity in the background EEG to reflect properties of the phasic peak and, therefore, to share important spatiotemporal features with phase-locked EEG activity.

These results demonstrate important limitations in analysis methods that focus on EEG and ERP activity within narrowly defined frequency bands. The primary drawback to such approaches, as we have discussed in detail, is that it is extremely difficult to determine whether observed oscillatory features of empirical data reflect true oscillatory phase resetting or whether they instead reflect frequency-specific components of phasic neural events. Future research might therefore profitably make use of existing techniques, such as wavelet and Fourier analyses, that permit the simultaneous analysis of time-varying spectral content across a broad range of frequencies. For example, whereas phasic events and synchronized oscillations may be indistinguishable within a narrow frequency band, they may differ substantially in their temporal and spectral profiles when analyzed across a broad range of frequencies. Thus, an important goal for future research will be to extend existing methods in order to develop more sophisticated, quantitative measures—based, for example, on wavelet or Fourier analyses—that might be sensitive to these more subtle distinctions.

We suggest that a fruitful approach for future research in this direction will be to apply newly developed analysis methods to simulated data sets of the kind used here. Because the nature of these data sets can be known and tightly controlled, they can be used to evaluate rigorously the effectiveness of the analysis methods in question. In the present research, we have shown that observed properties of empirical EEG data can be replicated in simulated data constructed in two very different ways, by synchronization of ongoing EEG oscillations and by the addition of classical phasic peaks. These results demonstrate that the analysis methods we have considered cannot provide unambiguous evidence of the presence of synchronized oscillations. Meanwhile, parallel research has used related simulation methods to explore weaknesses of analytic approaches previously used to support the classical view (Klimesch et al., 2006). Taken together, these results demonstrate the value of simulation studies in evaluating the efficacy of analysis methods that aim to distinguish between competing accounts of the neural basis of ERP waveforms.[2]

Overall, the present findings suggest that it remains open whether the ERN reflects phasic neural activity or the synchronization of ongoing EEG activity. Also uncertain is the degree to which this debate about the neural basis of the ERN will influence and inform debate about the functional significance of this component. On the one hand, to the extent that individual ERP components contain substantial power within a given frequency band, theories about these components will likely benefit from a consideration of research that has linked activity within those frequency bands with specific cognitive functions. In the context of the ERN, for example, one intriguing hypothesis is that this component might be related to frontal midline theta activity that has been consistently linked with working memory functions (Gevins, Smith, McEvoy, & Yu, 1997; Klimesch, 1999; Klimesch, Doppelmayr, Russegger, & Pachinger, 1996). On the other hand, the classical and synchronized oscillation views agree on the critical point that ERP peaks reflect neural events that are time-locked to the cognitive processes of interest—the theories only disagree as to whether these events cause phasic activity or phase resetting. Therefore, ERP components, and the ERN specifically, will remain useful tools for identifying and tracking the dynamics of neural events associated with psychological processes, irrespective of whether they are caused by phasic bursts of activity or oscillatory synchrony.

---

[2]To facilitate the use of our simulation methods in the evaluation of EEG analysis techniques, we have made available online our Matlab code for EEG data simulation, together with a brief tutorial, at the following URL: http://www.cs.bris.ac.uk/home/rafal/phasereset/.

REFERENCES

Başar, E. (1980). *EEG brain dynamics: Relation between EEG and brain evoked potentials.* Amsterdam: Elsevier.

Bogacz, R., Yeung, N., & Holroyd, C. B. (2002). *Detection of phase resetting in the electroencephalogram: An evaluation of methods.* Program No. 506.9. 2005 Abstract Viewer and Itinerary Planner. Washington, DC: Society for Neuroscience.

Botvinick, M. M., Braver, T. S., Carter, C. S., Barch, D. M., & Cohen, J. D. (2001). Evaluating the demand for control: Anterior cingulate cortex and crosstalk monitoring. *Psychological Review*, *108*, 624–652.

Brandt, M. E., Jansen, B. H., & Carbonari, J. P. (1991). Pre-stimulus spectral EEG patterns and the visual evoked response. *Electroencephalography and Clinical Neurophysiology*, *80*, 16–20.

Bush, G., Luu, P., & Posner, M. I. (2000). Cognitive and emotional influences in anterior cingulate cortex. *Trends in Cognitive Sciences*, *4*, 215–222.

Carter, C. S., Braver, T. S., Barch, D. M., Botvinick, M. M., Noll, D., & Cohen, J. D. (1998). Anterior cingulate cortex, error detection, and the online monitoring of performance. *Science*, *280*, 747–749.

Coles, M. G. H., Gratton, G., & Fabiani, M. (1990). Event-related brain potentials. In J. T. Cacioppo & L. G. Tassinary (Eds.), *Principles of psychophysiology: Physical, social and inferential elements* (pp. 413–455). Cambridge, UK: Cambridge University Press.

Coles, M. G. H., & Rugg, M. D. (1995). Event-related brain potentials: An introduction. In M. D. Rugg & M. G. H. Coles (Eds.), *Electrophysiology of mind: Event-related brain potentials and cognition* (pp. 1–26). Oxford: Oxford University Press.

Cooper, R., Winter, A. L., Crow, H. J., & Walter, W. G. (1965). Comparison of subcortical, cortical and scalp activity using chronically indwelling electrodes in man. *Electroencephalography and Clinical Neurophysiology*, *18*, 217–228.

Eriksen, B. A., & Eriksen, C. W. (1974). Effects of noise letters upon the identification of target letters in a non-search task. *Perception and Psychophysics*, *16*, 143–149.

Falkenstein, M., Hohnsbein, J., Hoorman, J., & Blanke, L. (1990). Effects of errors in choice reaction tasks on the ERP under focused and divided attention. In C. H. M. Brunia, A. W. K. Gaillard, & A. Kok (Eds.), *Psychophysiological brain research* (*Vol. 1*, pp. 192–195). Tilburg, the Netherlands: Tilburg University Press.

Gehring, W. J., Goss, B., Coles, M. G. H., Meyer, D. E., & Donchin, E. (1993). A neural system for error detection and compensation. *Psychological Science*, *4*, 385–390.

Gevins, A., Smith, M. E., McEvoy, L. K., & Yu, D. (1997). High-resolution EEG mapping of cortical activation related to working memory: Effects of task difficulty, type of processing, and practice. *Cerebral Cortex*, *7*, 374–385.

Goff, W. R., Allison, T., & Vaughan, H. G. (1978). The functional neuroanatomy of event related potentials. In E. Callaway, P. Tueting, & S. Koslow (Eds.), *Event-related brain potentials in man* (pp. 1–91). New York: Academic Press.

Gruber, W. R., Klimesch, W., Sauseng, P., & Doppelmayr, M. (2005). Alpha phase synchronization predicts p1 and n1 latency and amplitude size. *Cerebral Cortex*, *15*, 371–377.

Holroyd, C. B., & Coles, M. G. H. (2002). The neural basis of human error processing: Reinforcement learning, dopamine, and the error-related negativity. *Psychological Review*, *109*, 679–709.

Jansen, B. H., Agarwal, G., Hegde, A., & Boutros, N. N. (2003). Phase synchronization of the ongoing EEG and auditory EP generation. *Clinical Neurophysiology*, *114*, 79–85.

Jervis, B. W., Nichols, M. J., Johnson, T. E., Allen, E., & Hudson, N. R. (1983). A fundamental investigation of the composition of auditory evoked potentials. *IEEE Transactions on Biomedical Engineering*, *30*, 43–50.

Klimesch, W. (1999). EEG alpha and theta oscillations reflect cognitive and memory performance: A review and analysis. *Brain Research Reviews*, *29*, 169–195.

Klimesch, W., Doppelmayr, M., Russegger, H., & Pachinger, T. (1996). Theta band power in the human scalp EEG and the encoding of new information. *NeuroReport*, *7*, 1235–1240.

Klimesch, W., Hanslmayr, S., Sauseng, P., & Gruber, W. R. (2006). Distinguishing the evoked response from phase reset: A comment to Mäkinen et al. *NeuroImage*, *29*, 808–811.

Klimesch, W., Schack, B., Schabus, M., Doppelmayr, M., Gruber, W., & Sauseng, P. (2004). Phase-locked alpha and theta oscillations generate the p1-n1 complex and are related to memory performance. *Cognitive Brain Research*, *19*, 302–316.

Kruglikov, S. Y., & Schiff, S. J. (2003). Interplay of electroencephalogram phase and auditory-evoked neural activity. *Journal of Neuroscience*, *23*, 10122–10127.

Luu, P., & Tucker, D. M. (2001). Regulating action: Alternating activation of midline frontal and motor cortical networks. *Clinical Neurophysiology*, *112*, 1295–1306.

Luu, P., Tucker, D. M., & Makeig, S. (2004). Frontal midline theta and the error-related negativity: Neurophysiological mechanisms of action regulation. *Clinical Neurophysiology*, *115*, 1821–1835.

Makeig, S., Westerfield, M., Jung, T.-P., Enghoff, S., Townsend, J., Courchesne, E., et al. (2002). Dynamic brain sources of visual evoked responses. *Science*, *295*, 690–694.

Mäkinen, V., Tiitinen, H., & May, P. (2005). Auditory event-related responses are generated independently of ongoing brain activity. *NeuroImage*, *24*, 961–968.

Mazaheri, A., & Picton, T. W. (2005). EEG spectral dynamics during discrimination of auditory and visual targets. *Cognitive Brain Research*, *24*, 81–96.

McFarland, D. J., & Cacace, A. T. (2004). Separating stimulus-locked and unlocked components of the auditory event-related potential. *Hearing Research*, *193*, 111–120.

Pailing, P. E., Segalowitz, S. J., Dywan, J., & Davies, P. L. (2002). Error negativity and response control. *Psychophysiology*, *39*, 198–206.

Rabbitt, P. M. A. (1966). Error correction time without external error signals. *Nature*, *212*, 438.

Rabbitt, P. M. A. (2002). Consciousness is slower than you think. *Quarterly Journal of Experimental Psychology*, *55A*, 1081–1092.

Sayers, B. M., Beagley, H. A., & Henshall, W. R. (1974). The mechanism of auditory evoked EEG responses. *Nature*, *247*, 481–483.

Shah, A. S., Bressler, S. L., Knuth, K. H., Ding, M., Mehta, A. D., Ulbert, I., et al. (2004). Neural dynamics and the fundamental mechanisms of event-related brain potentials. *Cerebral Cortex*, *14*, 476–483.

Truccolo, W. A., Ding, M., Knuth, K. H., Nakamura, R., & Bressler, S. L. (2002). Trial-to-trial variability of cortical evoked responses: Implications for the analysis of functional connectivity. *Clinical Neurophysiology*, *113*, 206–226.

Vaughan, H. G. (1969). The relationship of brain activity to scalp recordings of event-related potentials. In E. Donchin & D. B. Lindsley (Eds.), *Average evoked potentials: Methods, results, and evaluations*. Washington, DC: U.S. Government Printing Office.

Yeung, N. (2004). Relating cognitive and affective theories of the error-related negativity. In M. Ullsperger & M. Falkenstein (Eds.), *Errors, conflicts, and the brain. Current opinions on performance monitoring* (pp. 63–70). Leipzig, Germany: Max Planck Institute of Cognitive Neuroscience.

Yeung, N., Bogacz, R., Holroyd, C. B., & Cohen, J. D. (2004). Detection of synchronized oscillations in the electroencephalogram: An evaluation of methods. *Psychophysiology*, *41*, 822–832.

Yeung, N., Botvinick, M. M., & Cohen, J. D. (2004). The neural basis of error detection: Conflict monitoring and the error-related negativity. *Psychological Review*, *111*, 931–959.